Scientific Research Publishing

Journal of Power and Energy Engineering, 2026, 14(1), 1-22
https://www.scirp.org/journal/jpee
ISSN Online: 2327-5901
ISSN Print: 2327-588X

Three-Dimensional CFD Analysis of Combustion and Emission Characteristics of Diesel/n-Butanol Blends Using CONVERGE

Joseph Lungu, Lennox Siwale, Rudolph Joe Kashinga, Bennet Siyingwa

School of Engineering, The Copperbelt University, Riverside Campus, Kitwe, Zambia
Email: josephlungu8512@gmail.com

How to cite this paper: Lungu, J., Siwale, L., Kashinga, R.J. and Siyingwa, B. (2026) Three-Dimensional CFD Analysis of Combustion and Emission Characteristics of Diesel/n-Butanol Blends Using CONVERGE. *Journal of Power and Energy Engineering*, **14**, 1-22.
https://doi.org/10.4236/jpee.2026.141001

Received: December 8, 2025
Accepted: January 16, 2026
Published: January 19, 2026

Abstract

This study presents a three-dimensional CFD investigation of the combustion and emission characteristics of diesel/n-butanol blended fuels (B5, B10, and B20, corresponding to 5%, 10%, and 20% n-butanol by volume, respectively) in a four-cylinder, 1.9 L Turbo-Direct Injection (TDI) diesel engine using CONVERGE CFD software. A detailed in-cylinder simulation was performed under engine loads of 25%, 50%, 75%, and 100% at a constant speed of 3000 rpm. The computational model incorporated spray breakup, turbulence, combustion, and emission sub-models, and was validated against experimental in-cylinder pressure and heat release rate data for conventional diesel (D2). In relation to experimental data, strong agreement, with maximum deviations below 8% was observed. Simulation results revealed that an increase in the n-butanol content has a direct influence on ignition delay, in-cylinder temperature, and heat release behavior due to enhanced oxygen availability and altered fuel atomization. Among the blends, B10 exhibited combustion characteristics most comparable to diesel, particularly at higher loads, while also demonstrating improved atomization and blend stability. Emission analysis showed that n-butanol blends tend to reduce CO, HC, and soot emissions across all loads, with B10 achieving up to 6% and 9% reductions in CO and HC, and an 8.4% reduction in soot at full load. Nevertheless, due to elevated oxygen content, a marginal increase in NOx (1.9%) was observed (for B10). Overall, the results indicate that moderate n-butanol blending offers a promising pathway for improving diesel engine combustion efficiency and emission performance without major modifications to engine operation.

Keywords

Combustion, n-Butanol, Diesel, Emission and Converge CFD

1. Introduction

Internal combustion engines have served as the primary power source for the transportation sector for more than a century, relying predominantly on hydrocarbon-based fuels. The growing demand for heavy-duty vehicles is projected to accelerate diesel fuel consumption at a faster rate than gasoline. Compression ignition engines, in particular, remain integral to transportation and power generation due to their high thermal efficiency, durability, and operational reliability, even as global energy systems shift towards more sustainable alternatives. The rapid expansion of the automotive industry and the rising number of vehicles have significantly contributed to elevated exhaust gas emissions, exacerbating environmental concerns and accelerating the depletion of fossil fuel reserves [1]. The use of petroleum oil in transportation significantly contributes to environmental deterioration through emissions such as nitrogen oxides (NOx), unburned hydrocarbons (UHC), carbon monoxide (CO), particulate matter (PM), and carbon dioxide (CO_2). These pollutants accumulate in the atmosphere, contributing to the greenhouse effect, global warming, and climate change. Oxygenates, including alcohols such as 1-butanol, have emerged as alternatives for improving the octane number and oxygen content in conventional fuels (gasoline, diesel) [2] [3].

Butanol has garnered significant research interest as a second-generation biofuel in recent years, being considered as a potential alternative to ethanol for replacing gasoline and diesel [4]. Until recently, it was less studied than ethanol or methanol. This was mainly due to its use in the food industry, undeveloped production from non-petroleum sources, and higher costs. However, interest in butanol has recently surged [5]. Butanol (C_4H_9OH) is a higher-chain alcohol with a four-carbon structure and exists in different isomers, which vary in physical properties based on the location of the hydroxyl (OH) group and the carbon chain structure [6]. These are 1-Butanol (also known as n-butanol), 2-butanol (also known as sec-butanol), isobutanol, and tert-butanol. 1-Butanol has a straight-chain structure with the alcohol (OH) group at the terminal carbon. 2-Butanol, on the other hand, has the hydroxyl group at an internal carbon. Isobutanol is a branched isomer with the OH group at the terminal carbon, and tert-butanol is a branched isomer with the OH group at an internal carbon. The different structures of butanol isomers directly impact their physical properties [6]. Laminar velocities tend to decrease in the order: 1-butanol, sec-butanol, isobutanol, and tert-butanol. Gu, Huang *et al.* (2010) state that the laminar flame speed, or fuel burning velocity, is a crucial parameter of a combustible mixture. This physicochemical property has a significant influence on combustion duration and performance in engines, as it directly affects the fuel burning rate in internal combustion engines, thereby impacting efficiency and emissions. The molecular structure of combustible mixtures, particularly the isomers of butanol, affects their laminar flame stability. 1-butanol exhibits the highest flame burning velocity. Other characteristics, such as functional groups, are widely known to significantly influence laminar burning velocity; branching (-CH3) decreases it, while the hydroxyl functional group (-OH)

attached to terminal carbon atoms is widely known to increase laminar velocity. Terminal C-H bonds tend to possess higher bond energies than those of inner C-H bonds. High bond energies hinder the H-abstraction reaction, leading to a lower reaction rate. Consequently, n-butanol, which mostly contains inner C-H bonds, has the highest laminar flame velocity, while tert-butanol has the lowest [2] [3]. A higher alcohol, such as butanol, can also be used as a blend component, owing to its properties, such as viscosity and cetane number (CN), which are closer to those of diesel than those of lower alcohols. The phase stability of the 1-butanol and diesel blends can also be improved by using higher alcohols such as propanol and pentanol. In contrast to ethanol, which is a lower alcohol, the miscibility of 1-butanol with diesel at a wide range of operating conditions is excellent. Furthermore, 1-butanol has a heat of vaporization of about 570 kJ/kg, while that of ethanol is about 900 kJ/kg. Therefore, the earlier initiation of 1-butanol evaporation may intensify the preparation of a combustible mixture and improve the auto-ignition of heavy volatile vegetable oil molecules in the blend [7]. Among the four butanol isomers, n-butanol (1-butanol) has been most extensively studied as a motor fuel in the literature and is, therefore, selected in this work, in line with previous studies on bio-butanol produced through ABE fermentation routes [8].

A number of experimental and theoretical research investigations have been published concerning diesel/n-butanol fuel engines. The focus has mostly been on the variation in combustion due to the effects of diesel fuel quantity, injection timing, injector nozzle design, injection pressure, and exhaust gas recirculation [9]. It is reported from the study by Rakopoulos *et al.* [9] that the impact of using blends of diesel fuel with 5% and 10% ethanol or 8% and 16% n-butanol, on the combustion cyclic variations in a turbocharged, heavy-duty, DI diesel engine, with tests at three loads and two speeds of 2000 rpm and 1500 rpm. Fuel consumption, exhaust smokiness, and exhaust regulated gas emissions such as nitrogen oxides, carbon monoxide, and total unburned hydrocarbons were measured. The results showed a decrease in CO and particulate matter while THC increased with no significant changes in NOx. Emissions reduction was also reported by Joy *et al.* [10] in their Emission analysis of diesel and butanol blends in a research on a diesel engine. The engine was fueled with diesel and two blends of butanol and diesel at atmospheric conditions, with D100, D90B10, and D80B20 as respective blends. The results showed that the chemical and physical properties of D100, D90B10, and D80B20 fall within the limits of ASTM standards. Another study by Huang *et al.* [11] reports that it is feasible and applicable for the blends with n-butanol to replace pure diesel as a fuel for a diesel engine. In their works, Rakopoulos *et al.* [12] [13] reported the reductions of smoke, nitrogen oxides (NOx), and carbon monoxide (CO) emissions, and increased hydrocarbons (HC) emissions. They concluded that it is advantageous to use n-butanol as a blend component, taking advantage of its relatively high cetane number and very good solubility in diesel.

Elucidation of combustion characteristics in internal combustion engines was

mostly done using controlled experiments [2] [7]-[12]. Nevertheless, experiments are expensive and time-consuming, hence the need for modeling and simulation using dedicated software. Zhang *et al.* [14] used AVL-FIRE 2013 to conduct simulations on low-water-level biodiesel emulsion fuel and pure biodiesel fuel. Madihi [15] used CONVERGE software to explore how altering the fuel supply time and injection rate influences the Reactivity-Controlled Compression Ignition concept. Others, such as Kim *et al.* [16], employed ANSYS FLUENT 2019R2 software to investigate how varying injection angles and positions impact the two-stroke diesel engine characteristics. These authors demonstrated that a 0.02 m injection position and a 40-degree injection angle result in improved engine performance. However, a 0.01 m injection position leads to reductions in NO, soot, CO_2, and other emissions. Yoon [17] studied the emissions and performance of blended fuels using the CFD software CONVERGE Studio 3.0 and found that simulation results were consistent with test results. Studies by Nurdiyana *et al.* [18] focused on dual fuel combustion using Converge CFD software. The engine was operated at 1800 rpm through two different load points in diesel and dual fuel operating modes. Motored pressure, combustion pressure, and net heat release rate (HRR) generated from the simulations compared well with the corresponding experimental results. Bousbaa *et al.* [19] carried out numerical study investigations on a diesel engine fueled by eucalyptus biofuel using Converge CFD software. The experiments were performed on a single cylinder direct injection diesel engine, with twice the load condition (50% and 90% of full load) at a constant speed of 1500 rpm, and a good agreement between the modelling and experimental data showed the accuracy in the numerical predictions in this work. Furthermore, Mao *et al.* used CONVERGE Studio 3.1.8 software to study Performance and Exhaust Emissions from Diesel Engines with Different Blending Ratios of Biofuels. Thus, CFD software enables the simulation and analysis of diesel engine combustion.

Despite the extensive studies on oxygenated fuels, there remains insufficient CFD-based understanding of how n-butanol/diesel blends influence in-cylinder combustion and emission behavior under varying engine loads. Existing literature [3] [7] often relies on limited experimental conditions or lacks validated three-dimensional CFD models capable of resolving spray breakup, ignition delay, Nox-soot formation, and temperature evolution in modern TDI engines. Furthermore, the effects of low and moderate n-butanol blend ratios at high engine speeds (3000 rpm) are still inadequately characterized. Therefore, this study undertakes to validate load-dependent CFD-based investigations of the combustion of diesel/n-butanol blends, in order to elucidate their combustion and emission characteristics.

2. Materials and Methods

In this study, the experimental test results used to validate CFD-based simulations were conducted on a four-cylinder, 1.9 L, 66 kW Turbo-Direct Injection (TDI) diesel engine. The engine was equipped with a turbocharger and integrated with

the necessary sensors and actuators to ensure stable and controlled operation. All tests were performed at a constant engine speed of 3000 rpm under four load conditions: 25%, 50%, 75%, and 100%. The engine parameters are given in Table 1, while the operating conditions for the reference fuel (D2) are given in Table 2 below.

Table 1. Engine parameters.

Engine Model	Audi 1.9 L, TDI
Capacity	1896 cm^3
Bore	79.5 mm
Stroke	95.5 mm
Compression Ratio	19.5:1
Maximum Power	66 kW, at 4000 rpm
Maximum Torque	202 Nm at 1900 rpm
Fuel System	Direct injection with an electronic distributor-type injector pump (Bosch VP37 type)
Combustion System	Bowl-in-piston chamber with 5 holes 180 bar opening pressure injector

Source: [3] [7].

Table 2. Operating conditions of the engine for diesel fuel (D2).

Load (%)	Torque (Nm)	BSEC (MJ/kWh)
25	184.6	12.39
50	136.5	10.30
75	91	9.82
100	45.5	9.24

Source: [3] [7].

3. Numerical Modeling and Simulation

3.1. Computational Modeling

The numerical simulations are carried out using the available software CONVERGE CFD code. This was achieved through a professional development program called CONVERGE Explore. CONVERGE 3.1 is a Computational Fluid Dynamics tool for the simulation of three-dimensional, incompressible/compressible, chemically reacting transient fluid flows in complex geometries with stationary or moving surfaces [19]. CONVERGE has the capability to handle any number of species and chemical reactions, as well as transient liquid sprays, and laminar or turbulent flows. Its sub-models are originally developed for petroleum-based fuels, such as gasoline and diesel. The 3D simulations are performed using the Eulerian-Lagrangian approach. Different sub-models are included in CONVERGE 3.1. software such as spray injection, atomization and breakup, droplet collision, coa-

lescence, and turbulence. The gas-phase flow field is described using the Favre-Averaged Navier-Stokes equations. Details regarding the code and how it works have been mentioned by K. J. Richards [19] [20].

The 3-D simulations were performed using the RANS approach, considering compressible fluid, non-stationary regime, and ideal gas assumption in the computational fluid dynamics (CFD) software CONVERGE. It incorporates models for spray injection, atomization and breakup, turbulence, droplet collision, and coalescence. The gas-phase flow field is described using the Favre-Averaged Navier-Stokes equations in conjunction with the RNG k-ε turbulence model, which includes source terms for the effects of dispersed phase on gas-phase turbulence. These equations are solved using a finite volume solver. Kelvin-Helmholtz (KH) and Rayleigh-Taylor (RT) models are used to predict the primary and secondary breakup of the computational parcels [20]. For combustion, the multi-scale CTC (Characteristic Time Combustion) model associated with the Shell ignition model [20] is used. Currently, CONVERGE includes sub-models for both soot and NOx production. For NOx prediction, the extended Zeldovich NOx model [20] is adopted. Finally, the Hiroyasu soot model is used for soot prediction [19] [20].

3.2. Three-Dimensional CFD Model

The three-dimensional CFD model was developed by constructing the engine cylinder geometry in SolidWorks 2018. A bowl-in-piston combustion chamber was designed to enhance mixture formation and combustion efficiency in a direct-injection compression ignition engine. The finalized geometry was exported in STL format and imported into CONVERGE Studio for pre-processing. A full 360˚ sector model was generated in CONVERGE Studio, with the piston, cylinder head, and liner defined as the primary boundary surfaces. The geometry is shown in **Figure 1**.

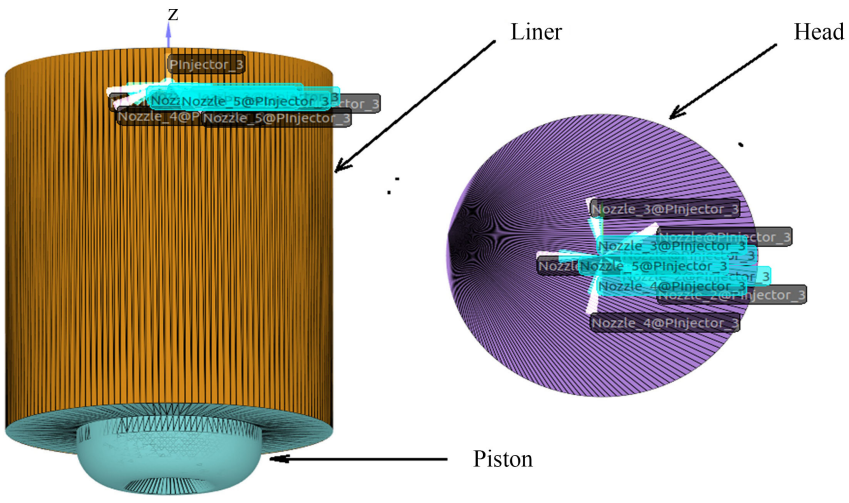

Figure 1. 3D geometry generated in CONVERGE Studio.

3.3. Adaptive Mesh Refinement

CONVERGE is a revolutionary computational fluid dynamics (CFD) program that eliminates the grid generation bottleneck from the simulation. Unlike many CFD programs, CONVERGE automatically generates a perfectly orthogonal, structured grid at runtime based on simple, user-defined grid control parameters. This grid generation method completely eliminates the need to manually generate a grid. The mesh was created such that the boundary was flagged and adjusted to have the real geometry (bore, stroke, etc.). The adaptive mesh refinement (AMR) technique in CONVERGE enables local mesh refinement according to temperature, velocity, and species gradients [20]. The base grid resolution is specified in an input file, thus allowing for grid resolution studies to be performed without making separate meshes. The geometry volume is always correctly calculated, allowing for extremely coarse meshes to be used while setting up a case. In the actual study, the AMR is activated for velocity and the temperature at start −11.5˚C CA BTDC and end at 140˚C CA ATDC. The AMR algorithm automatically adds the setting where the flow field is most under-resolved or where the sub-grid is the largest. Consequently, the cell size and the total number of cells are not constant and change over the simulation process. In addition, CONVERGE offers many other features to expedite the setup process and to ensure that your simulations are as computationally efficient as possible [19] [20].

4. Boundary and Initial Conditions

Table 3. Initial conditions at 25% load.

Temperature	420 K
Pressure	134,000 Pa
Turbulent Kinetic Energy	62.0271 m^2/s^2
Turbulent Dissipation	17,183.4 m^2/s^3

Boundary conditions play a crucial role in defining the model's scope and ensuring the accurate representation of physical phenomena in computational simulations. They explain the effects of these models before going into detail about new behaviors and connecting models from various physics theoretical frameworks [1]. Diesel engine CFD simulations typically begin at intake valve closing (IVC) and end at exhaust valve closing (EVC), with initial conditions such as swirl ratio defined prior to computation. In this study, a closed-cycle simulation was performed from −147˚ crank angle degrees (CAD) to 135˚ CAD, covering the compression and expansion strokes and focusing exclusively on in-cylinder processes. Three wall boundary types were applied, with the piston defined as a translating boundary and the cylinder head and liner treated as stationary, smooth walls. A standard logarithmic wall-law formulation was employed to model the near-wall turbulent boundary layer and calculate the tangential stress components. These initial and boundary condition assumptions play a critical role in establishing ac-

curate in-cylinder flow and combustion predictions. Figure 1 shows the piston, head, and liner of the combustion chamber. The initial conditions of the engine while running at 3000 rpm and 25% load are shown in Table 3, while the specifications of the injection data are summarized in Table 4.

Table 4. Fuel system specifications.

Number of Nozzle Holes	5
Nozzle Hole Diameter	21 mm
Spray Angle	150˚C
Start of Injection	1.8 deg BTDC
Injection Duration	9 deg
Total Injected Mass	11.71 mg
Injection Pressure	178.899 bar

Source: [3] [7].

Chemical Reaction Mechanism

In this study, the gas-phase component of diesel was represented using n-heptane due to its cetane number and ignition characteristics, which closely match those of conventional diesel fuel. The liquid phases of diesel and n-butanol were modeled using the Diesel2 and 1-butanol property datasets available in the CONVERGE fuel library. Due to the close similarity in cetane number between n-heptane and diesel fuel, n-heptane is commonly employed as a surrogate fuel in diesel engine simulation studies. Most detailed chemical kinetic models for diesel surrogate combustion are based on the n-heptane oxidation mechanisms developed by Lawrence Livermore National Laboratory [21] [22]. However, because these detailed mechanisms are computationally intensive for coupled CFD-chemistry calculations, the reduced n-heptane-butanol-PAH mechanism proposed by Hu and Wang [23] was adopted in the present study. The reduced n-heptane/n-butanol/PAH mechanism developed by Hu and Wang [23] has been validated for ignition delay, spray combustion, and soot formation under engine-relevant conditions. The mechanism has been validated against ignition delay measurements from shock-tube studies, HCCI engine data, and diesel spray combustion experiments, demonstrating reliable predictive capability under engine-relevant conditions. A phenomenological multistep soot model was integrated with the n-heptane/n-butanol/PAH mechanism to enable accurate prediction of soot formation in lifted flames and diesel engine environments. This framework also captures the influence of n-butanol as an oxygenated additive and its impact on combustion chemistry and emission formation [23]. The mechanism is verified by the experimental data of the shock tube, the constant volume combustion bomb, and the engine, and it is able to predict the process of fuel combustion and the generation of the emissions [22]. The kinetic mechanism contains 4 elements, 74 species, and 349 reactions. The properties of diesel and n-butanol are given in Table 5.

Table 5. Properties of diesel and n-butanol.

Fuel Properties	Diesel Fuel	n-Butanol C_4H_9OH
Density at 20˚C, kg/m^3	823.20	811.95
Cetane Number	54.6	~17
Lower Calorific Value, MJ/kg	42.92	33.94
Kinematic Viscosity at 20˚C, mPas	3.4[a]	3.6[b]
Boiling Point, ˚C	180 - 360	118
Latent Heat of Evaporation, kJ/kg	250	585
Oxygen, %wt	0	21.6
Stoichiometric Air-Fuel Ratio	15.0	11.2
Molecular Weight	170	74

Source: [3] [7].

5. Results and Discussion

5.1. Model Validation

In this study, an in-cylinder CFD simulation was performed using diesel as the reference fuel, and the model was validated to ensure the reliability and accuracy of the numerical predictions. Validation was carried out by comparing simulation results with experimental data reported in the literature [3] [7] at a constant engine speed of 3000 rpm under four load conditions: 25%, 50%, 75%, and 100%. The model's predictive capability was assessed by evaluating key combustion metrics—specifically in-cylinder pressure and heat release rate (HRR)—which demonstrated good agreement with the corresponding experimental measurements. **Figure 2** and **Figure 3** illustrate the simulation results for diesel combustion process, and provide a comparative analysis of in-cylinder pressure and heat release rate between the present work study and experimental data.

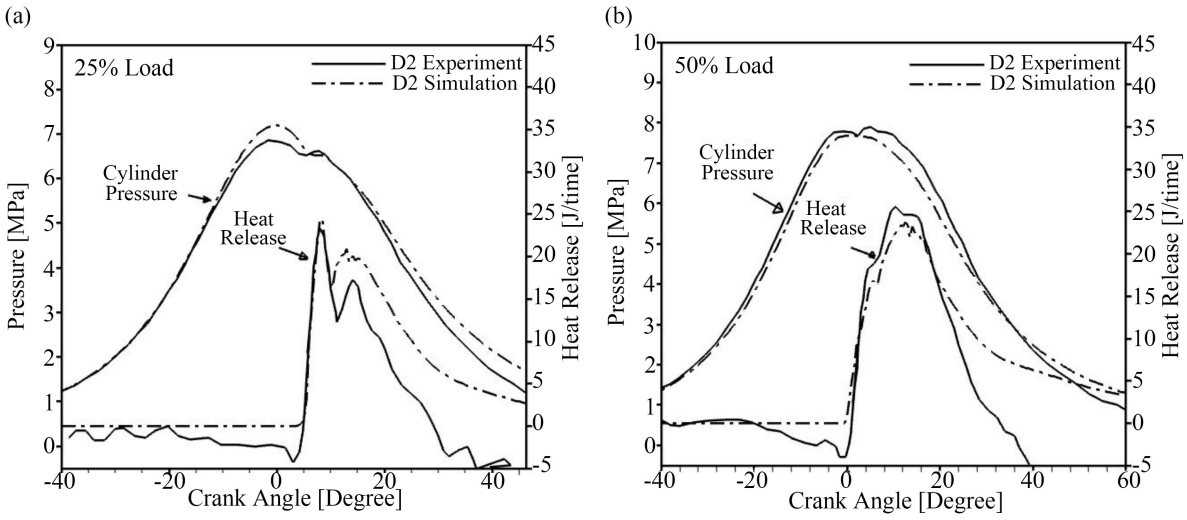

Figure 2. In-cylinder pressure and heat release rate (HRR) at 25% and 50% load.

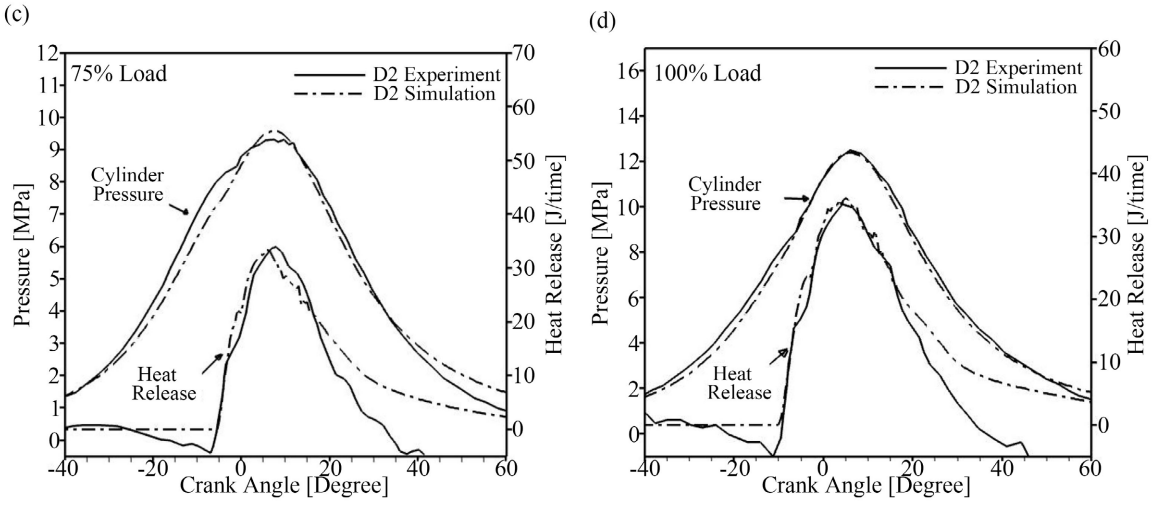

Figure 3. In-cylinder pressure and heat release rate at 75% and 100% load.

5.2. Variation in Maximum Pressure and Heat Release Rate (HRR)

A percentage error analysis was performed to quantify the deviation between the simulated and experimental results. This evaluation provides a measure of how closely the numerical predictions capture the experimentally observed combustion behavior. At 25% load and 3000 rpm, the experimental peak cylinder pressure was 6.63 MPa, compared to 7.19 MPa predicted by the simulation, corresponding to a 7.8% deviation. Under the same conditions, the maximum experimental heat release rate was 23.33 J/time, while the simulation produced 24.33 J/time, yielding a percentage error of 1.5%. These results indicate that the model provides satisfactory agreement with experimental data. **Table 6** below summarizes the variations in maximum pressure and heat release rate for 25%, 50%, 75% and 100% engine load.

The model's accuracy was confirmed by examining the results of the test pertaining to the in-cylinder pressure and heat release rate. Variations in maximum pressure and heat release rate have been identified and compared with existing experimental results [3] [7], indicating that the current model can be used for additional analysis.

Table 6. Variation in maximum pressure and HRR.

Load (%)	Experimental P (MPa)	Simulation P (MPa)	Maximum Variation (%)	Experiment HRR (J/T)	Simulation HRR (J/T)	Maximum Variation (%)
25	6.63	7.19	7.8	23.31	24.33	4.2
50	7.80	7.68	1.5	25.51	23.66	7.3
75	9.32	9.58	2.7	34.00	33.30	2.1
100	12.5	12.38	0.96	35.18	36.02	2.3

5.3. Simulation of Combustion Characteristics

5.3.1. In-Cylinder Pressure

A comprehensive evaluation of the in-cylinder pressure traces was performed to

gain deeper insights into the combustion development, heat release characteristics, thermal efficiency, and overall performance of the engine under varying load conditions. In compression-ignition engines, in-cylinder pressure varies significantly with crank angle due to changes in-cylinder volume, the rate of fuel-air mixing, heat release, and heat transfer to the surrounding walls. **Figure 2** and **Figure 3** present the simulated pressure profiles for diesel at 25%, 50%, 75%, and 100% engine loads at a constant speed of 3000 rpm.

At 25% load, the peak in-cylinder pressure reached 6.87 MPa at −1.65 CAD, corresponding to the onset of rapid premixed combustion. As the load increased, the peak pressure values rose consistently, reaching 7.90 MPa at 4.96 CAD for 50% load, 9.32 MPa at 9.78 CAD for 75% load, and 12.5 MPa at 6.03 CAD for full-load operation. This incremental rise in peak pressure is primarily attributable to the increased quantity of injected fuel with load, which enhances the total chemical energy available for combustion. Higher fuel mass results in a greater heat release rate, thereby elevating both peak pressure and the rate of pressure rise.

The shift in peak pressure location with load also reflects changes in mixing-controlled combustion. At higher loads, the injection duration increases, resulting in improved mixture formation and more energetic combustion phasing. Additionally, increasing the load tends to intensify turbulence levels inside the combustion chamber, thereby promoting more rapid mixing and accelerating the combustion process.

Thermal efficiency increases with load due to the higher heat release and improved combustion completeness associated with elevated cylinder temperatures. Furthermore, complete combustion strongly depends on proper fuel-air mixing; hence, sufficient air availability becomes increasingly crucial as more fuel is injected per cycle. At higher loads, although more fuel is delivered, the engine simultaneously draws in a larger air mass due to boosted intake pressure (from the turbocharger), supporting more complete combustion and contributing to the observed rise in peak in-cylinder pressure.

5.3.2. Mean Temperature

In-cylinder pressure, temperature, and heat release characteristics are important in assessing compression ignition engines' performance deviations. Due to differences in their chemical properties, different fuels may have different thermal characteristics, which may be close to the characteristics of the design fuel (in this case, fossil diesel) but may be different. When blending different fuels, in order to achieve better economic and environmental performance, it is necessary to assess the deviation of the pressure, pressure rise, heat release, and in-cylinder temperature characteristics from those of fossil diesel (the design fuel) [24].

In this study, diesel fuel was blended with n-butanol at volumetric fractions of 5%, 10%, and 20% (B5, B10, and B20), and the resulting combustion behavior was compared with baseline diesel (D2). Simulations were performed at a constant engine speed of 3000 rpm under four load conditions: 25%, 50%, 75%, and 100%. **Figures 4-9** present the corresponding in-cylinder temperature profiles and con-

tour plots, enabling a comprehensive assessment of how blend ratio and load influence combustion temperature distribution.

At 25% load, D2 exhibited the highest peak in-cylinder temperature (1407 K), while B5 produced the lowest (1403 K). This slight reduction in temperature for lower butanol ratios is linked to the fixed start of injection (1.8˚ ATDC) and short injection duration (9˚ CA), which limit air-fuel mixing at low load. Reduced mixing time, combined with the lower reactivity of n-butanol, leads to a marginal decrease in combustion temperature. B10 and B20 generated peak temperatures of 1405 K and 1407 K, respectively, indicating that increasing n-butanol concentration compensates for mixing limitations by supplying additional oxygen that enhances local combustion efficiency.

As engine load increased, the peak in-cylinder temperature rose for all fuels due to increased fuel mass, higher heat release, and intensified turbulence, which improves atomization and fuel-air mixing. At 50% load, maximum temperatures for D2, B10, and B20 were 1814 K, 1807 K, and 1814 K, respectively. By 75% load, the peak temperatures for D2, B10, and B20 converged closely at 2090 K, 2090 K, and 2093 K. The close alignment of these temperature curves indicates similar combustion phasing and heat release behavior across the blends at intermediate loads.

At full load, B20 recorded the highest peak temperature (2056 K), whereas D2, B5, and B10 reached 2051 K, 2043 K, and 2048 K, respectively. The slight temperature increase observed with B20 is attributed to its higher oxygen content, which enhances combustion completeness when fuel injection quantity is maximized. Across all loads, B10 consistently produced temperature profiles closest to D2, suggesting that a 10% n-butanol blend retains thermochemical characteristics similar to conventional diesel while offering improved oxygenation and combustion stabilization. This behavior could be explained by the physical and chemical properties of n-butanol when blended with diesel. The incorporation of n-butanol significantly enhanced the combustion process due to its high oxygen content, which further increased the combustion efficiency and subsequently reduced ignition delay. Furthermore, the results show that the temperature curves for cylinder pressure and HRR curves at the beginning and end of combustion exhibited a convergence, suggesting a similar end of combustion among the fuels [25].

Figures 6-9 present the in-cylinder temperature contour maps for D2, B5, B10, and B20 at 25%, 50%, 75%, and 100% load. These spatial temperature distributions provide a visual representation of the instantaneous high-temperature regions within the combustion chamber. The contour maps show that temperature intensity and distribution broaden with increasing load for all fuels, reflecting higher heat release and stronger turbulence. Among the blends, B10 consistently exhibits temperature patterns closest to D2, while B20 shows slightly more extensive high-temperature zones at higher loads due to its enhanced oxygen content. Overall, the contour results support the trends observed in the temperature curves and confirm the influence of blend ratio and load on combustion development.

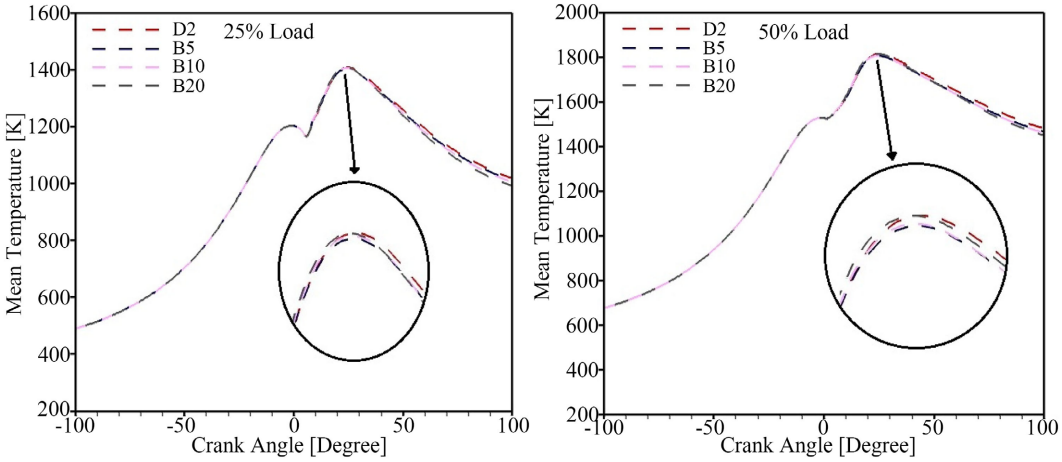

Figure 4. In-cylinder combustion temperature of diesel fuel blends at 25% and 50% load.

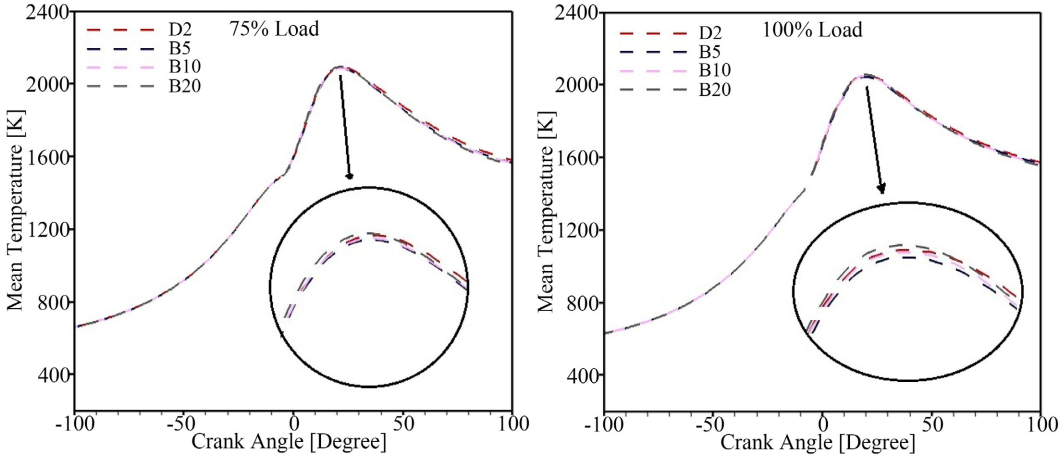

Figure 5. In-cylinder combustion temperature of diesel fuel blends at 75% and 100% load.

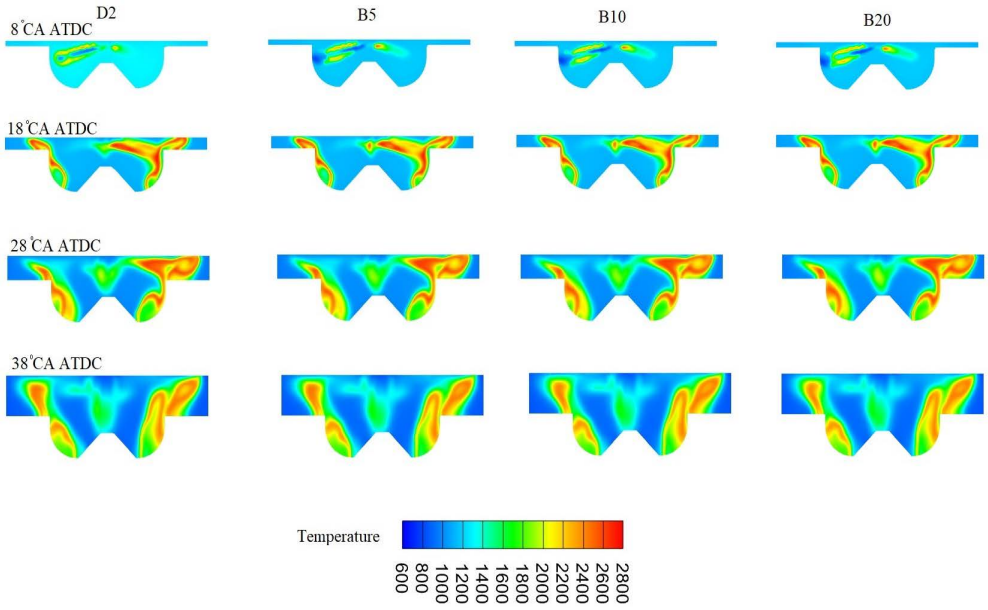

Figure 6. In-cylinder temperature contour maps for diesel fuel blends at 25% load.

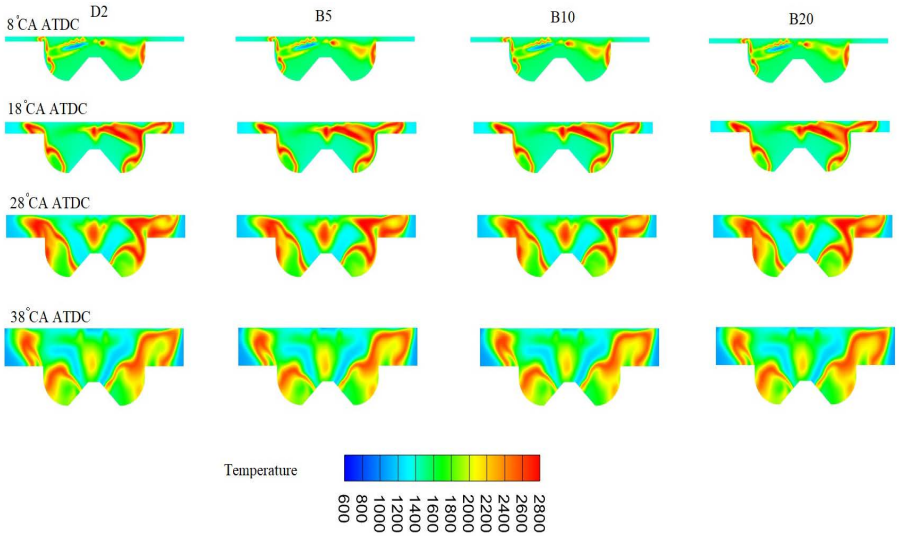

Figure 7. In-cylinder temperature contour maps for diesel fuel blends at 50% load.

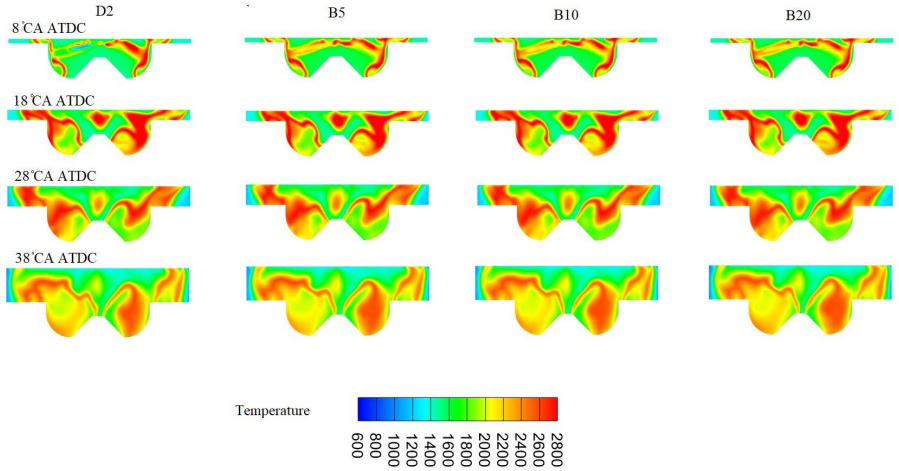

Figure 8. In-cylinder temperature contour maps for diesel fuel blends at 75% load.

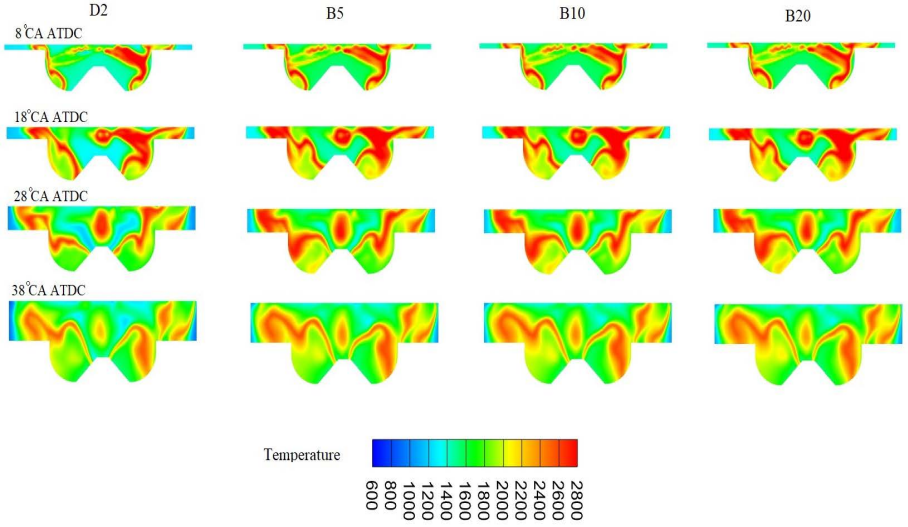

Figure 9. In-cylinder temperature contour maps for diesel fuel blends at 100% load.

5.3.3. Heat Release Rate

The heat release rate is a significant combustion parameter derived from the application of the first law of thermodynamics to the pressure of the gases within the cylinder [26]. This is because the HRR indicates the combustion rate of the blended fuels. The HRR is used to identify the start of combustion, the fraction of fuel burned in the premixed mode, and differences in combustion rates of fuels [27]. At full load, the maximum peak heat release rates (HRR) for B5, B10, and B20 were 35.5, 35.4, and 35.8 J/time, respectively, compared with 36.1 J/time for the baseline diesel (D2). Among the blends, B10 exhibited the lowest HRR, which can be attributed to a deterioration in spray atomization at this blend ratio. Poorer fuel breakup reduces the available surface area for evaporation and mixing, leading to a less efficient premixed combustion phase and consequently lower HRR. This reduced mixing quality also delays the oxidation of unburned hydrocarbons, increasing the likelihood of incomplete combustion before the exhaust valve opens, a trend similarly reported by Nour *et al.* [28].

At 25% and 50% loads, all n-butanol blends (B5, B10, B20) produced higher peak HRR values than D2. This behavior is consistent with the enhanced premixed combustion facilitated by the additional oxygen content in n-butanol, which accelerates early-stage combustion and improves flame propagation. According to Nour *et al.* [28], higher peak HRR values at low and intermediate loads typically indicate more efficient fuel-air preparation and improved premixed combustion (**Figure 10**).

At 75% load, the maximum HRR values for D2, B5, B10, and B20 were 33.3, 33.3, 33.2, and 34.1 J/time, respectively. The close alignment of these values demonstrates similar combustion phasing among all fuels at this load point. The HRR peaks occurring near top dead center (TDC) indicate efficient conversion of chemical energy into mechanical work, reflecting optimal combustion timing across the tested blends (**Figure 10**).

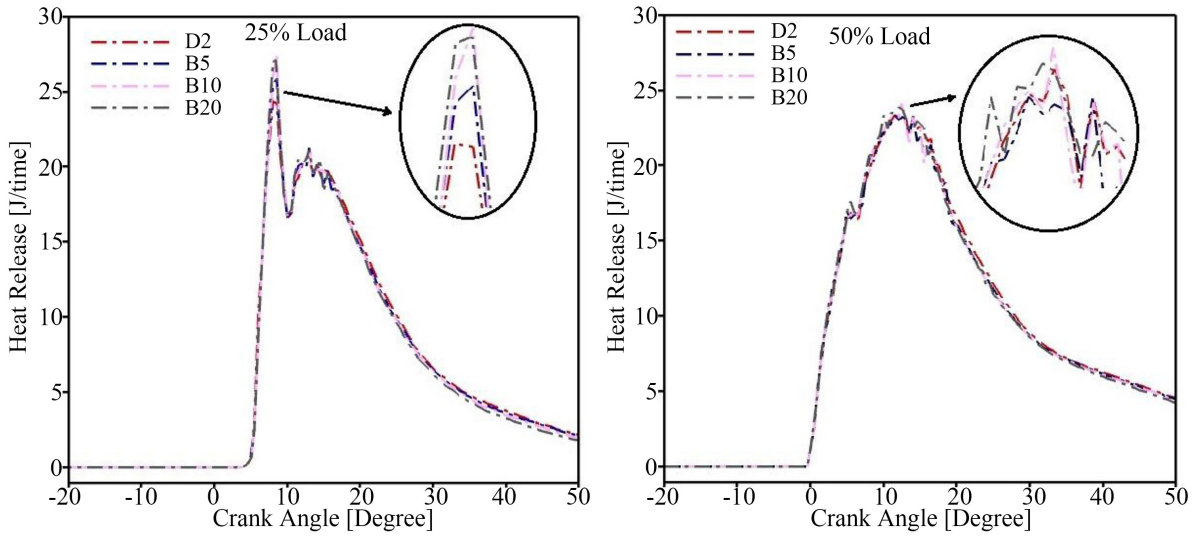

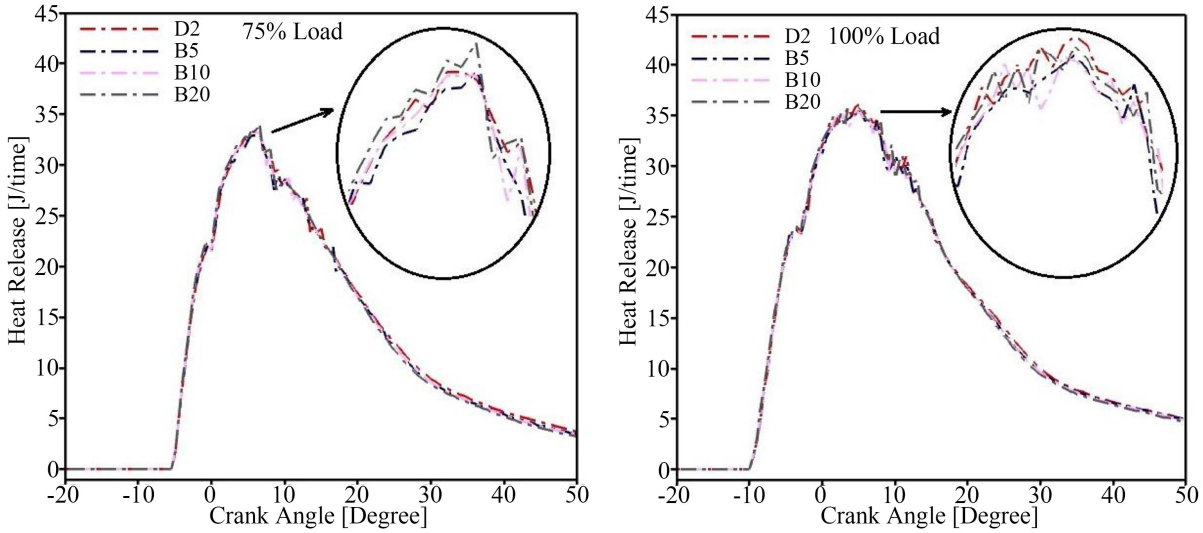

Figure 10. Heat release rates of the diesel fuel mixture at 25%, 50%, 75%, and 100% load.

5.4. Simulation Results of In-Cylinder Exhaust Emissions

5.4.1. Mass of CO and HC Emissions

In diesel engines, the production of CO and HC is primarily a result of incomplete combustion caused by uneven fuel-air mixing and localized oxygen deficiency [29]. **Figure 11** shows the simulation results on the mass of CO and HC during the combustion process, which was observed at EVC. CO is a colorless and odorless toxic gas that, at high concentrations, prevents hemoglobin in the blood from effectively binding to oxygen, leading to oxygen deprivation. Therefore, it is highly hazardous. Owing to their potential involvement in atmospheric chemical reactions that contribute to the generation of pollutants like ozone and fine particles, HCs have negative implications for both human health and the natural environment [25] [29]. It can be noted from **Figure 11** that the blends emitted a lower concentration of CO and HC in comparison with diesel. At 25% load, CO and HC emissions were at their lowest for all fuels, and the addition of n-butanol further reduced CO and HC concentrations across all fuel blends. The addition of n-butanol reduced fuel density and viscosity, thereby improving fuel volatility and atomization. Additionally, the high oxygen content of n-butanol-rich fuels improved the overall oxygen concentration, prevented localized oxygen deficiency, and enhanced the combustion efficiency, thereby reducing the CO and HC.

Under 50% and 75% load conditions, the decreasing and then increasing concentrations of CO and HC emissions trend stemming from the incorporation of n-butanol may be due to conflicting factors. The elevated LHV of n-butanol lowers the cylinder temperature, potentially causing incomplete combustion, whereas the improved combustion environment resulting from the substantial oxygen content within n-butanol can reduce the emissions. These conflicting phenomena increased CO and HC emissions when 5% n-butanol was added at 50% and 75% load. Since alcohol fuels like n-butanol have a higher latent heat of vaporization than diesel, more heat is normally absorbed during vaporization. This leads to a

lowering of the in-cylinder temperatures and an extension of the ignition delay period, which tends to reduce combustion efficiency and results in an increase in products such as CO and HC, due to incomplete combustion [30].

Under 100% load conditions, a similar trend was observed, with the decreasing and then increasing concentrations of CO and HC. As reported by Çakmak *et al.* [31], the increase in the concentration of CO and HC emissions can be explained by the poor volatility and higher viscosity. At 100% load, B20 was observed to exhibit the lowest concentration of CO and HC emissions.

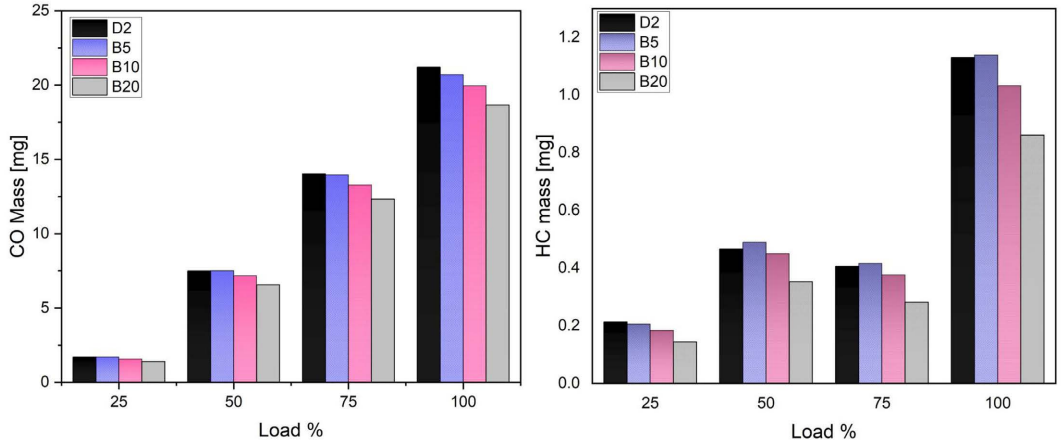

Figure 11. Mass of CO and HC emissions from 25% to 100% Load.

5.4.2. Mass of NOx and Soot Emissions

NOx poses risks to human health and the environment, necessitating its reduction in accordance with relevant regulations. In the context of diesel engines, NOx is predominantly formed through the Zeldovich mechanism. Because of the presence of 78.6% nitrogen gas (N_2) and 20.95% oxygen (O_2) in air, nitrogen and oxygen atoms combine at elevated temperatures, leading to NOx generation [25] [32]. Thus, NOx emissions are primarily influenced by flame temperature, duration, and levels of oxygen [25] [33]. As engine load increased, combustion temperatures intensified, resulting in higher NOx emissions for all tested fuels. Under low-load conditions, conventional diesel (D2) exhibited the lowest NOx levels due to a reduction in in-cylinder temperatures and slower combustion rates. However, the incorporation of n-butanol led to a consistent increase in NOx emissions for B5, B10, and B20 across all operating conditions. This rise is primarily attributed to the oxygen content of n-butanol, which enhances combustion completeness and elevates local flame temperatures—conditions favorable for thermal NOx formation. Although n-butanol has a lower LHV than diesel, the blended fuels exhibited shorter ignition delays due to factors such as decreased droplet size and variations in cetane number (CN). As a result, the mixture remained at elevated temperatures for a longer duration, further increasing NOx formation, consistent with observations reported by other researchers.

Soot emissions arise in compression-ignition engines from the incomplete ox-

idation of fuel in oxygen-deficient regions following high-temperature evaporation. Excess unburned fuel that does not oxidize completely is ultimately emitted from the engine [33]. Key factors influencing soot formation include the degree of fuel-air premixing, injection timing, spray atomization, and the availability of oxygen. As shown in Figure 12, soot emissions decreased with the addition of biodiesel and n-butanol, although the influence of n-butanol alone remained relatively modest. Because n-butanol has lower viscosity and higher volatility compared with biodiesel, its inclusion directly improves spray atomization and evaporation, thereby reducing fuel-rich regions within the cylinder and lowering soot precursor formation. However, the reduced LHV of n-butanol also slightly decreases combustion temperature, which can limit soot oxidation. These competing effects explain the relatively subtle—but consistent—reduction in soot emissions for the n-butanol blends. At full load, the engine injects a larger amount of fuel to achieve higher output power, creating more fuel-rich zones and therefore producing the highest soot levels [34]. Nonetheless, under all load conditions, the addition of n-butanol (B5, B10, B20) resulted in lower soot emissions compared with diesel.

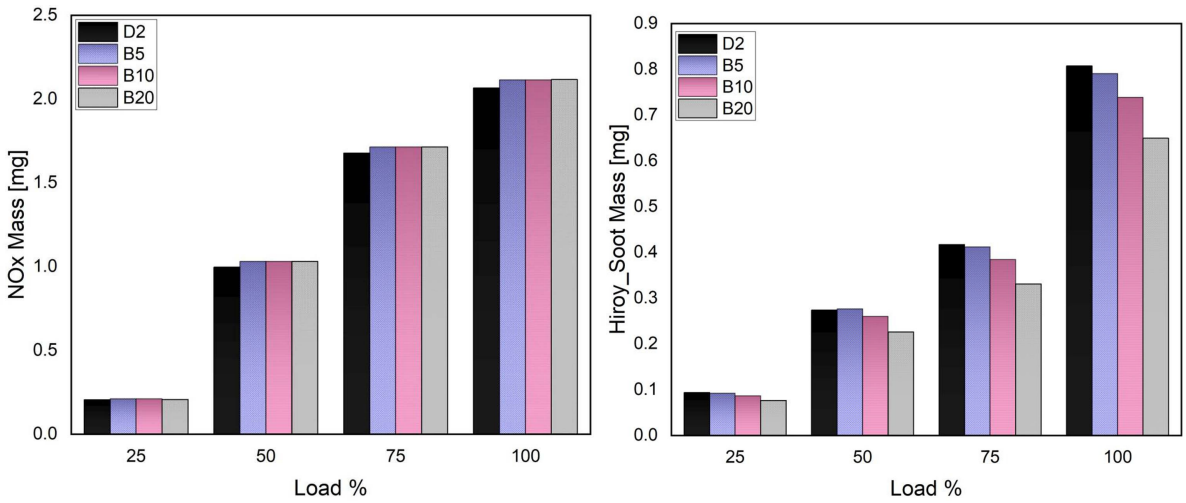

Figure 12. Mass of NOx and soot emissions from 75% to 100% Load.

6. Limitations of the Study

The present study has a few inherent limitations that may affect the generality of the results: 1) the simulations employs a specific reduced chemical kinetics mechanism (n-heptane-butanol-PAH), which, although validated, may not fully capture all reaction pathways and intermediate species present in real diesel/n-butanol combustion; 2) diesel is represented by a single-component surrogate (n-heptane), which simplifies the complex hydrocarbon composition of commercial diesel and may influence predictions of ignition, heat release, and emissions; 3) the analysis is restricted to selected engine operating conditions and blend ratios. As such, extension to a broader range of conditions and multi-component surrogate

fuels could provide more comprehensive insights into combustion and emission behavior; and iv) the simulations are restricted to the closed-cycle portion of the engine, *i.e.*, a full 720˚ engine cycle simulation, including intake and exhaust processes, would be required to capture the complete engine dynamics and further validate the predicted combustion and emission behavior.

7. Conclusions

This work conducted a detailed CFD-based evaluation of diesel/n-butanol blends (B5, B10, B20) in a 1.9 L TDI diesel engine and compared/validated simulation results with experimental combustion measurements. Based on the analysis of in-cylinder pressure, temperature, HRR, and emissions, the following conclusions were established:

1) The developed CFD model exhibited strong agreement with experimental pressure and HRR data across all operating conditions, confirming the accuracy and robustness of the simulation framework.

2) The fuel blend B10 demonstrated combustion characteristics most comparable to diesel, achieving peak temperatures of 2048 K at full load and a HRR of 33.2 J/time at 75% load, indicating proper phasing and efficient heat release.

3) Among all the fuel blends, B10 delivered the most favorable overall performance due to improved fuel atomization, enhanced evaporation behavior, and superior blend stability compared to B5 and B20.

4) Emission analysis revealed that the fuel blend B10 exhibited a reduction in in-cylinder CO by 5% - 6% and HC by 7% - 9% at medium and high loads relative to diesel. At full load, B10 produced a minor 1.9% increase in NOx but achieved a significant 8.4% reduction in soot, demonstrating a beneficial NOx-soot trade-off characteristic of oxygenated fuels.

Overall, the findings identify B10 as the optimal fuel blend, offering improved combustion performance and lower emissions while maintaining close similarity to diesel operation under all tested conditions. This blend also demonstrates potential as a drop-in fuel for existing diesel engines, providing environmental and operational benefits without requiring significant hardware modifications.

Conflicts of Interest

The authors declare no conflicts of interest regarding the publication of this paper.

References

[1] Pranta, M.H. and Cho, H.M. (2025) Numerical Analysis of Diesel Engine Combustion and Performance with Single-Component Surrogate Fuel. *Energies*, **18**, Article 1082. https://doi.org/10.3390/en18051082

[2] Lungu, J., Siwale, L. and Kashinga, R.J. (2024) Performance, Combustion and Emission Characteristics of Oxygenated Diesel in DI Engines: A Critical Review. *Journal of Power and Energy Engineering*, **12**, 16-49. https://doi.org/10.4236/jpee.2024.126002

[3] Siwale, L.Z., Kolesnikov, P.A., Bereczky, P.A. and Mbarawa, M. (2012) Effect of Ox-

ygenated Additives in Conventional Fuels for Reciprocating Internal Combustion Engines on Performance Combustion and Emission Characteristics. Ph.D. Thesis, Tshwane University of Technology.

[4] Hui, X., Niemeyer, K.E., Brady, K.B. and Sung, C. (2016) Reduced Chemistry for Butanol Isomers at Engine-Relevant Conditions. *Energy & Fuels*, **31**, 867-881. https://doi.org/10.1021/acs.energyfuels.6b01857

[5] Rajesh Kumar, B. and Saravanan, S. (2016) Use of Higher Alcohol Biofuels in Diesel Engines: A Review. *Renewable and Sustainable Energy Reviews*, **60**, 84-115. https://doi.org/10.1016/j.rser.2016.01.085

[6] Wallner, T., Miers, S.A. and McConnell, S. (2009) A Comparison of Ethanol and Butanol as Oxygenates Using a Direct-Injection, Spark-Ignition Engine. *Journal of Engineering for Gas Turbines and Power*, **131**, Article 032802. https://doi.org/10.1115/1.3043810

[7] Lujaji, F., Kristóf, L., Bereczky, A. and Mbarawa, M. (2011) Experimental Investigation of Fuel Properties, Engine Performance, Combustion and Emissions of Blends Containing Croton Oil, Butanol, and Diesel on a CI Engine. *Fuel*, **90**, 505-510. https://doi.org/10.1016/j.fuel.2010.10.004

[8] Obergruber, M., Hönig, V., Procházka, P., Kučerová, V., Kotek, M., Bouček, J., *et al.* (2021) Physicochemical Properties of Biobutanol as an Advanced Biofuel. *Materials*, **14**, Article 914. https://doi.org/10.3390/ma14040914

[9] Rakopoulos, C.D., Rakopoulos, D.C., Kosmadakis, G.M. and Papagiannakis, R.G. (2019) Experimental Comparative Assessment of Butanol or Ethanol Diesel-Fuel Extenders Impact on Combustion Features, Cyclic Irregularity, and Regulated Emissions Balance in Heavy-Duty Diesel Engine. *Energy*, **174**, 1145-1157. https://doi.org/10.1016/j.energy.2019.03.063

[10] Joy, N., Balan, K.N., Nagappan, B. and Justin Abraham baby, S. (2020) Emission Analysis of Diesel and Butanol Blends in Research Diesel Engine. *Petroleum Science and Technology*, **38**, 289-296. https://doi.org/10.1080/10916466.2019.1702680

[11] Zhou, X., Qian, W., Pan, M., Huang, R., Xu, L. and Yin, J. (2020) Potential of n-Butanol/Diesel Blends for CI Engines under Post Injection Strategy and Different EGR Rates Conditions. *Energy Conversion and Management*, **204**, Article 112329. https://doi.org/10.1016/j.enconman.2019.112329

[12] Rakopoulos, D.C., Rakopoulos, C.D., Giakoumis, E.G., Dimaratos, A.M. and Kyritsis, D.C. (2010) Effects of Butanol-Diesel Fuel Blends on the Performance and Emissions of a High-Speed DI Diesel Engine. *Energy Conversion and Management*, **51**, 1989-1997. https://doi.org/10.1016/j.enconman.2010.02.032

[13] Rakopoulos, D.C., Rakopoulos, C.D., Hountalas, D.T., Kakaras, E.C., Giakoumis, E.G. and Papagiannakis, R.G. (2010) Investigation of the Performance and Emissions of Bus Engine Operating on Butanol/Diesel Fuel Blends. *Fuel*, **89**, 2781-2790. https://doi.org/10.1016/j.fuel.2010.03.047

[14] Zhang, Z., E, J., Chen, J., Zhu, H., Zhao, X., Han, D., *et al.* (2019) Effects of Low-Level Water Addition on Spray, Combustion and Emission Characteristics of a Medium Speed Diesel Engine Fueled with Biodiesel Fuel. *Fuel*, **239**, 245-262. https://doi.org/10.1016/j.fuel.2018.11.019

[15] Madihi, R., Pourfallah, M., Gholinia, M., Armin, M. and Ghadi, A.Z. (2022) Thermofluids Analysis of Combustion, Emissions, and Energy in a Biodiesel ($C_{11}H_{22}O_2$)/Natural Gas Heavy-Duty Engine with RCCI Mode (Part II: Fuel Injection Time/Fuel Injection Rate). *International Journal of Thermofluids*, **16**, Article 100200. https://doi.org/10.1016/j.ijft.2022.100200

[16] Kim, J., Lee, W., Pham, V.C. and Choi, J. (2022) A Numerical Study on Fuel Injection Optimization for a ME-GI Dual-Fuel Marine Engine Based on CFD Analysis. *Applied Sciences*, **12**, Article 3614. https://doi.org/10.3390/app12073614

[17] Yoon, S.K. (2022) Investigation on the Combustion and Emission Characteristics in a Diesel Engine Fueled with Diesel-Ethanol Blends. *Applied Sciences*, **12**, Article 9980. https://doi.org/10.3390/app12199980

[18] Nurdiyana, W., Mansor, W. and Olsen, D.B. (2016) Computational Modeling of Diesel and Dual Fuel Combustion Using Converge CFD Software. *ARPN Journal of Engineering and Applied Sciences*, **11**, 13697-13707.

[19] Bousbaa, H., Tarabet, L., Khatir, N. and Liazid, A. (2020) Numerical Study on a Diesel Engine Fueled by Eucalyptus Biofuel Using Converge CFD Software. *JSC Technologies*, **2**, 106-119.

[20] Richards, E., Senecal K.J. and Pomraning, P.K. (2024) CONVERGE Manual v3.1. CONVERGENT Science, Madison, WI, 1-1454.

[21] Curran, H.J., Gaffuri, P., Pitz, W.J. and Westbrook, C.K. (1998) A Comprehensive Modeling Study of N-Heptane Oxidation. *Combustion and Flame*, **114**, 149-177. https://doi.org/10.1016/s0010-2180(97)00282-4

[22] Wang, H. and Liu, W. (2015) Simulation Studies of Diesel Engine Combustion Characteristics with Oxygen Enriched Air. *Journal of Power and Energy Engineering*, **3**, 15-23. https://doi.org/10.4236/jpee.2015.38002

[23] Wang, H., Deneys Reitz, R., Yao, M., Yang, B., Jiao, Q. and Qiu, L. (2013) Development of an *n*-Heptane-*n*-Butanol-PAH Mechanism and Its Application for Combustion and Soot Prediction. *Combustion and Flame*, **160**, 504-519. https://doi.org/10.1016/j.combustflame.2012.11.017

[24] Rimkus, A. and Žaglinskis, J. (2024) Study of the Combustion Characteristics of a Compression Ignition Engine Fueled with a Biogas-Hydrogen Mixture and Biodiesel. *Journal of Marine Science and Engineering*, **12**, Article 2192. https://doi.org/10.3390/jmse12122192

[25] Mao, C., Wei, J., Wu, X. and Ukaew, A. (2024) Performance and Exhaust Emissions from Diesel Engines with Different Blending Ratios of Biofuels. *Processes*, **12**, Article 501. https://doi.org/10.3390/pr12030501

[26] Nanthagopal, K., Ashok, B., Saravanan, B., Patel, D., Sudarshan, B. and Aaditya Ramasamy, R. (2018) An Assessment on the Effects of 1-Pentanol and 1-Butanol as Additives with *Calophyllum inophyllum* Biodiesel. *Energy Conversion and Management*, **158**, 70-80. https://doi.org/10.1016/j.enconman.2017.12.048

[27] Raheman, H. and Padhee, D. (2015) Combustion Characteristics of Diesel Engine Using Producer Gas and Blends of Jatropha Methyl Ester with Diesel in Mixed Fuel Mode. *International Journal of Renewable Energy Development*, **3**, 228-235. https://doi.org/10.14710/ijred.3.3.228-235

[28] Nour, M., Attia, A.M.A. and Nada, S.A. (2019) Combustion, Performance and Emission Analysis of Diesel Engine Fuelled by Higher Alcohols (Butanol, Octanol and Heptanol)/Diesel Blends. *Energy Conversion and Management*, **185**, 313-329. https://doi.org/10.1016/j.enconman.2019.01.105

[29] Rakopoulos, C.D., Rakopoulos, D.C., Giakoumis, E.G. and Kyritsis, D.C. (2011) The Combustion of *n*-Butanol/Diesel Fuel Blends and Its Cyclic Variability in a Direct Injection Diesel Engine. *Proceedings of the Institution of Mechanical Engineers, Part A: Journal of Power and Energy*, **225**, 289-308. https://doi.org/10.1177/2041296710394256

[30] Zheng, F. and Cho, H.M. (2024) Exploring the Effects of Synergistic Combustion of

Alcohols and Biodiesel on Combustion Performance and Emissions of Diesel Engines: A Review. *Energies*, **17**, Article 6274. https://doi.org/10.3390/en17246274

[31] Çakmak, A. and Özcan, H. (2020) Evaluation of Glycerol Tert-Butyl Ethers as Renewable Fuel Additive. *International Journal of Automotive Engineering and Technologies*, **9**, 66-75. https://doi.org/10.18245/ijaet.655168

[32] Singh, R., Singh, S. and Kumar, M. (2020) Impact of n-Butanol as an Additive with Eucalyptus Biodiesel-Diesel Blends on the Performance and Emission Parameters of the Diesel Engine. *Fuel*, **277**, Article 118178. https://doi.org/10.1016/j.fuel.2020.118178

[33] Huang, Y., Li, Y., Luo, K. and Wang, J. (2020) Biodiesel/Butanol Blends as a Pure Biofuel Excluding Fossil Fuels: Effects on Diesel Engine Combustion, Performance, and Emission Characteristics. *Proceedings of the Institution of Mechanical Engineers, Part D: Journal of Automobile Engineering*, **234**, 2988-3000. https://doi.org/10.1177/0954407020916989

[34] Atmanli, A. (2016) Comparative Analyses of Diesel-Waste Oil Biodiesel and Propanol, n-Butanol or 1-Pentanol Blends in a Diesel Engine. *Fuel*, **176**, 209-215. https://doi.org/10.1016/j.fuel.2016.02.076